Modrich, P., & Rubin, R. A. (1977) *J. Biol. Chem. 252*, 7273–7278.
Nerdal, W., Hare, D. R., & Reid, B. R. (1989) *Biochemistry 28*, 10008–10021.
Newman, P. C., Nwosu, V. U., Williams, D. M., Cosstick, R., Seela, F., & Connolly, B. A. (1990a) *Biochemistry 29*, 9891–9901.
Newman, P. C., Williams, D. M., Cosstick, R., Seela, F., & Connolly, B. A. (1990b) *Biochemistry 29*, 9902–9909.
Otinowski, Z., Schevitz, R. W., Zhang, R.-G., Lawson, C. L., Joachimiak, A., *Marmorstein*, R. Q., Luisi, B. F., & Sigler, P. B. (1988) *Nature 355*, 321–329.
Petruska, J., Goodman, M. F., Boosalis, M. S., Sowers, L. C., Cheong, C., & Tinoco, I. (1988) *Proc. Natl. Acad. Sci. U.S.A. 85*, 6252–6256.
Reich, N. O., & Everett, E. (1990) *J. Biol. Chem. 265*, 8929–8934.
Reich, N. O., & Mashhoon, N. (1990) *J. Biol. Chem. 265*, 8966–8970.
Reich, N. O., & Danzitz, M. (1991) *Nucleic Acids Res. 19* (23), 6587–6594.
Reich, N. O., & Mashhoon, N. (1991) *Biochemistry 30*, 2933–2939.
Rubin, R. A., & Modrich, P. (1977) *J. Biol. Chem. 252*, 7265–7272.
Saenger, W., Hunter, W. N., & Kennard, O. (1986) *Nature 324*, 385–388.
Seela, F., & Kehne, A. (1987) *Biochemistry 26*, 2232–2238.
Shortle, D., Meeker, A. K., & Freire, E. (1988) *Biochemistry 27*, 4761–4768.
Takeda, Y., Sarai, A., & Rivera, V. M. (1989) *Proc. Natl. Acad. Sci. U.S.A. 86*, 439–443.
Wharton, R. P., & Ptashne, M. (1987) *Nature 326*, 888–891.
Wing, R., Drew, H. R., Takano, T., Broka, C., Tanaka, S., Itakura, K., & Dickerson, R. E. (1980) *Nature 287*, 755–758.
Wolberger, C., Dong, Y., Ptashne, M., & Harrison, S. C. (1988) *Nature 335*, 789–795.
Wolfes, H., Alves, J., Fliess, A., Geiger, R., & Pingoud, A. (1986) *Nucleic Acids Res. 14*, 9063–9080.
Zappia, V., Galletti, P., Porcelli, M., Manna, C., & Ragione, F. D. (1980) *J. Chromatogr. 189*, 399–405.

Structural Basis of Human Erythrocyte Glucose Transporter Function: pH Effects on Intrinsic Fluorescence†

James J. Chin, Byung H. Jhun, and Chan Y. Jung*
Department of Biophysical Sciences, State University of New York at Buffalo, and the Biophysical Laboratory, Veterans Administration Medical Center, Buffalo, New York 14215
Received August 20, 1991; Revised Manuscript Received December 4, 1991

ABSTRACT: The effects of pH on the intrinsic fluorescence of purified human erythrocyte glucose transporter (HEGT) were studied to deduce the structure and the ligand-induced dynamics of this protein. D-Glucose increases tryptophan fluorescence of HEGT at a 320-nm peak with a concomitant reduction in a 350-nm peak, suggesting that glucose shifts a tryptophan residue from a polar to a nonpolar environment. Cytochalasin B or forskolin, on the other hand, only produces a reduction at the 350-nm peak. The pH titration of the intrinsic fluorescence of HEGT revealed that at least two tryptophan residues are quenched, one with a pK_a of 5.5, the other with a pK_a of 8.2, indicating involvement of histidine and cysteine protonation, respectively. D-Glucose abolishes both of these quenchings. Cytochalasin B or forskolin, on the other hand, abolishes the histidine quenching but not the cysteine quenching and induces a new pH quenching with a pK_a of about 4, implicating involvement of a carboxyl group. These results, together with the known primary structure and the transmembrane disposition of this protein, predict the dynamic interactions between Trp388 and His337, Trp412 and Cys347, and Trp412 and Glu380, depending on liganded state of HEGT, and suggest the importance of the transmembrane helices 9, 10, and 11 in transport function.

A family of specific transmembrane proteins facilitates the movement of glucose across the plasma membrane in animal cells (Mueckler et al., 1985; Birmbaum et al., 1986; Charron et al., 1989; James et al., 1989). Four tissue-specific isoforms are identified in this family, including the erythrocyte type (GLUT-1), liver and pancreatic β-cell type (GLUT-2), and muscle and fat cell type (GLUT-4) (Bell et al., 1990). All of these isoforms have 12 transmembrane α-helices (TMH 1–12, numbered in sequence from the N-terminal to the C-terminal ends) of highly conserved amino acid sequences (Bell et al., 1990) thought to form a transmembrane aqueous channel for glucose (Mueckler et al., 1985; Jung et al., 1986; Chin et al., 1986). These isoforms also show similar non-membrane domain structures, which may play important roles in tissue–specific regulations of transporter function (Bell et al., 1990).

GLUT-1 of human erythrocytes is the only isoform that is available as a purified and functional protein (HEGT)[1] in this family (Kasahara & Hinkle, 1977; Baldwin et al. 1982; Rampal et al., 1985). HEGT has been used extensively for the biochemical and biophysical characterization of this iso-

† This work was supported in part by National Institute of Health Grant DK13376 and by the Veterans Administration Medical Center, Buffalo, NY.
* Address correspondence to this author at the Veterans Administration Medical Center.

[1] Abbreviations: HEGT, human erythrocyte glucose transporter; TMH, transmembrane α helix.

0006-2960/92/0431-1945$03.00/0

form (Sogin & Hinkle, 1978; Baldwin et al., 1981; Wheeler & Hinkle, 1981; Gorga & Lienhard, 1982; Deziel et al., 1985; Chin et al., 1986, 1987; Jung et al., 1986; Carruthers, 1986a,b; Rampal & Jung, 1987; Cairns et al., 1987; Holman & Rees, 1987; Gibbs et al., 1988; Applemann & Lienhard, 1989; Pawagi & Deber, 1990). A detailed description of the tertiary structure and dynamics of this protein, however, is not currently available. Because of the common structural motif shared by all the isoforms, such a detailed structural description of HEGT would provide understanding of not only the transport function of this isoform but also those of all the isoforms in this family.

The intrinsic protein fluorescence due to its endogenous tryptophan(s) is know to be sensitive to local microenvironments and has served as a useful probe in studying protein tertiary structure and its dynamics (Chen & Edelhoch, 1975). For HEGT, quenching of the intrinsic fluorescence by ligands has been studied to describe protein dynamics induced by transporter substrates and inhibitors (Gorga & Lienhard, 1982; Carruthers, 1986a,b; Applemann & Lienhard, 1989; Pawagi & Deber, 1990). These studies have suggested that up to two of the six trypotphan residues in HEGT are exposed and that the binding of substrates and inhibitors reduces the quantum yield of these exposed tryptophan residues.

In the present study, we studied the effects of pH on the intrinsic fluorescence of HEGT in the absence and in the presence of D-glucose, cytochalasin B, and forskolin and demonstrated that the fluorescence is quenched by changes in pH with pK_a's of approximately 5.5, 8.2, and 4.0, depending on the presence and absence of ligands. The results suggest that there are direct interactions between TMH 9, 10, and 11 in HEGT and that D-glucose relaxes these interactions while the inhibitors enhance the interactions.

Materials and Methods

Purification and Reconstitution of HEGT. HEGT in liposomes were prepared by DEAE-cellulose chromatography of octyl β-glucoside-solubilized membranes and reconstituted by removing detergents as described (Rampal et al., 1986). The proteoliposome preparation was sonicated using a bath sonicator for 10 min at 4 °C to reduce vesicle size to less than 100 nm without loss of cytochalasin B binding activity. Cytochalasin B binding activity was assayed as described using [^{3}H]cytochalasin B as a tracer (Pinkofsky et al., 1978). Only those preparations that showed a specific cytochalasin B binding activity of more than 15 nmol/mg of protein were used. The protein was quantitated by Lowry assay (Lowry et al., 1951), using bovine serum albumin as a standard. Phospholipids were quantitated by phosphate determination (Bartlett, 1959). Spectroscopic samples were prepared by diluting HEGT proteoliposomes to 12–13 μg protein/mL. For the pH 3–7 titration, samples were prepared without buffer. Samples in the pH 7–9 range contained 50 mM Tris-HCl.

Fluorescence Measurements. Fluorescence measurements were performed on a SLM 8000C spectrofluorometer (Aminco-Bowman) without polarizers, using version 2.2 software. The instrument was set to the photon counting mode for optimum sensitivity with excitation and emission slit widths of 2 and 2 nm, respectively. Spectra were typically scanned two or three times using 1-nm step intervals with an integration rate of 0.5 s/nm. Excitation at 295 nm was used to minimize the contribution of tyrosine fluorescence (Weber & Teale, 1965). To maximize tyrosine fluorescence, excitation at 276 nm was used. Reported spectra fluorescence intensities are relative values based on the ratio mode of two photon detectors and are uncorrected for emission wavelength photon detector response. Experiments were performed with samples maintained at 25 °C in a circulating water bath. Samples were constantly stirred using the SLM magnetic curvette stirrer. To reduce sample variation and increase reproducibility, ligands were introduced by adding them sequentially in aliquots directly to the sample without removing the cell from the holder. For pH titration experiments, the sample pH was titrated by HCl and measured directly in the cell by a pH electrode. For the pH 7–9 samples which contained 50 mM Tris-HCl, the pH was measured individually. The repeated scanning of samples was corrected for fluorescence loss, presumably due to photolysis of tryptophan or tyrosine (Applemann & Lienhard, 1985). Under maximum exposure conditions of 2 h at 276 nm, samples showed less than 15% fluorescence decay. In all instances, scans were completed below the maximum exposure conditions. Monoexponential correction of fluorescence loss for controls and samples was adequate to maintain less than 1% variation from the original scan over the entire emission range, indicating that the photolysis of the residues was nonselective. Buffer and ligand fluorescence as well as the sample dilution artifact were corrected. Fluorescence changes due to titration of the sample volume up to 25% were correctable to less than 1% variation from initial scans. A correction of inner filter effects due to addition of ligands was applied as suggested (Parker, 1968). The fluorescence of a control sample containing L-glucose was not significantly different from that of samples in buffer, as reported by others (Gorga & Lienhard, 1982; Pawagi & Deber, 1990).

Molecular Modeling of TMH. The transmembrane helix structure was simulated using the program SYBYL software (version 5.2) by Tripos on a VAXII-750 computer equipped with an Evans and Sutherland PS 340 molecular graphics terminal. The helical structures of TMH 9 (His337–Leu358) and TMH 11 (Ala402–Phe422) were drawn on the basis of cDNA sequence of GLUT1 (Mueckler et al., 1985). In order to predict the structure of TMH 10, which contains proline, a well-known helix breaker, an α-helical structure was drawn from Ile369 to Val381, and the secondary structure of the remaining residues, Gly382–Phe389, was predicted on the basis of Bayes statistics (Maxfield & Scheraga, 1976; Gibral et al., 1987).

Results

Intrinsic Fluorescence of HEGT. The intrinsic fluorescence of HEGT at pH 7.4 was first examined. Typical emission maxima of tryptophan are at around 350 nm in water and at 310–324 nm in nonpolar protein regions (Konev, 1967). When excited at 295 nm, HEGT displayed a fluorescence emission peak centered at about 333 nm (Figure 1). This would indicate that the six tryptophan residues in HEGT are distributed between nonpolar and polar environments.

When an excess of D-glucose or cytocholasin B was added, the emission peak shifted to the shorter wavelengths by 2–4 nm, and the fluorescence was quenched strongly at the longer wavelength (Figure 1A). This effect has been noted previously (Gorga & Lienhard, 1982; Carruthers, 1986a; Pawagi & Deber, 1990). Using the SLM fluorometer and lower concentrations of HEGT proteoliposomes to minimize excitation beam scattering, however, we depict here (Figure 1) for the first time that the binding of D-glucose also induces a significant increase in fluorescence at shorter wavelengths from the peak. This is typical of tryptophan shift from a polar to a nonpolar environment. This effect is modest at pH 7.4 but became much more evident at pH 5.0 (Figure 1B) where HEGT retains its transport function.[2] Excitation at 276 nm

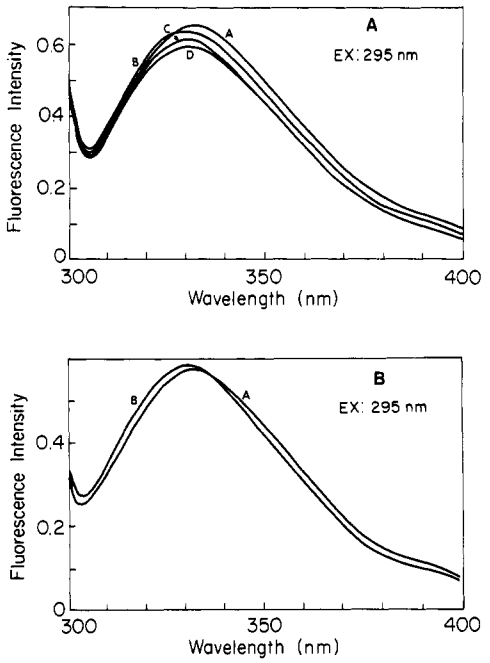

FIGURE 1: Fluorescence emission spectra of HEGT excitation at 295 nm, in the absence (A) or in the presence of 400 mM D-glucose (B), 15 μM cytochalasin B (C), or 400 mM D-glucose plus 15 μM cytochalasin B (D). Fluorescence was measured at pH 7.4 (panel A) and 5.0 (panel B).

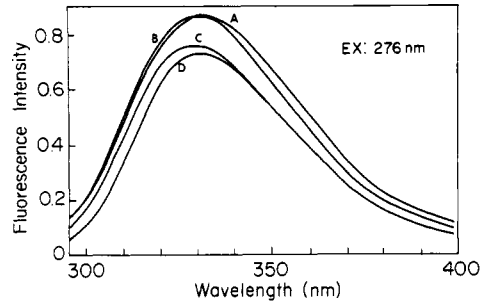

FIGURE 2: Fluorescence emission spectra of HEGT excited at 276 nm, in the absence (A) or in the presence of 400 mM D-gluocse (B), 15 μM cytochalasin B (C), and 400 mM D-glucose plus 15 μM cytochalasin B (D).

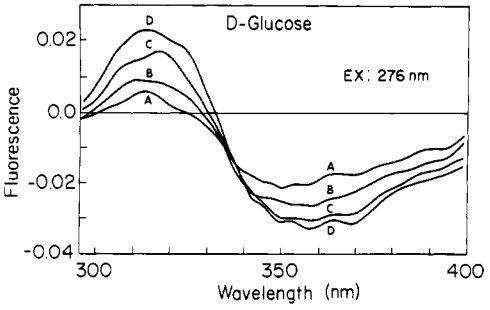

FIGURE 3: Difference spectra of HEGT between the absence and the presence of D-glucose. The glucose concentrations were (A) 10, (B) 20, (C) 50, and (D) 200 mM.

(Figure 2) did not affect the magnitude of these fluorescence changes appreciably (compare Figures 1A and 2), indicating that it is mostly tryptophan fluorescence and that the contribution by tyrosine is minimal. The difference spectra of this sample at pH 7.4 (Figure 3 and Table I) shows a 2–3% emission increase at a maximum between 310 and 320 nm, in association with a 3–4% decrease at a maximum between

[2] Unpublished results by J. J. Chin, A. L. Rampal, and C. Y. Jung.

Table I: Analysis of Substrate- and Inhibitor-Induced Changes in the Intrinsic Fluorescence of HEGT as a Function of Ligand Concentration[a]

	decrease in 360-nm peak		increase in 315-nm peak	
ligands	Δ_T[b]	K_D (M)	Δ_T	K_D (M)
D-glucose	0.033	6.5×10^{-3}	0.027	35.7×10
cytochalasin B	0.085	2.7×10^{-7}	ND[c]	
forskolin	0.067	5.2×10^{-6}	ND	

[a] The analyses were made on the basis of double-reciprocal plots using difference spectra of Figures 3 and 4. Excitation was at 276 nm. Ligand-induced intrinsic fluorescence changes Δ at ligand concentration L were quantitated at 315 and 360 nm from difference spectra plotted according to the relationship $1/\Delta = 1/\Delta_T + K_D/\Delta_T(1/L)$, where Δ_T and K_D denote the maximal fluorescence change and a constant related to ligand-binding affinity to the protein, respectively. [b] In fractions of total fluorescence. [c] Not detectable.

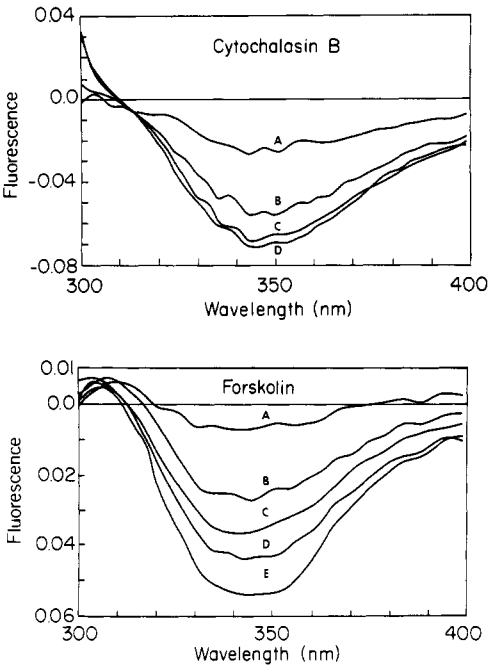

FIGURE 4: Difference spectra of HEGT between the absence and the presence of cytochalasin B (panel A, top) and forskolin (panel B, bottom), all are at 295-nm excitation. Cytochalasin B concentrations were (A) 125 nM, (B) 375 nM, (C) 750 nM, and (D) 3.5 μM. Forskolin concentrations were (A) 0.5, (B) 2.6, (C) 5.2, (D) 8, and (E) 16 μM.

350 and 360 nm. Since these spectra were obtained at 276-nm excitation, this suggests either an enviromental shift of tryptophan or a decrease in energy transfer from tyrosine to tryptophan. Both maxima are saturable at high concentrations of D-glucose, showing apparent half-maxima at two distinct D-glucose concentrations K_D for 360- and 315-nm emissions (Table I). Interestingly, these K_D values are very similar to the K_M values reported for the GLUT-1 transport function of human erythrocytes in zero-trans and in equilibrium exchange measurements, respectively [see Stein (1986) and Carruthers (1990)]. L-Glucose did not produce these effects (not illustrated).

In contrast to the D-glucose effect, the difference spectra (excitation at 296 nm) of HEGT liganded with cytochalasin B or forskolin (Figure 4) show only the reduction with a single saturable maxima at 340–350 nm without any concomitant increase at shorter wavelengths. Similar results were also obtained with difference spectra at 276-nm excitation (not show). This would indicate that the quenching induced by these inhibitor is due to a reduction in the quantum yield of

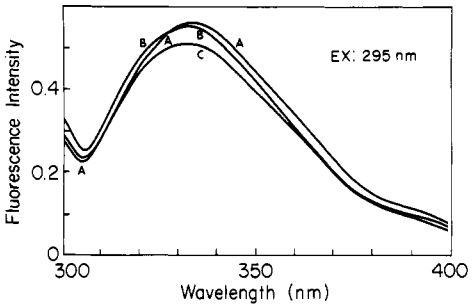

FIGURE 5: Fluorescence emission spectra of HEGT measured with excitation at 295 nm in the absence (A) and in the presence of 3.5 μM forskolin plus 400 mM D-glucose (B), or 3.5 μM forskolin alone (C).

an exposed tryptophan (Gorga & Lienhard, 1982; Pawagi & Deber, 1990) and there was no indication for a shift of tryptophan residues from polar to nonpolar environments. Analysis of the dose dependencies of the quenching by these inhibitors revealed apparent affinities (Table I) that are very similar to the affinities reported for the transport inhibition by these inhibitors, (2–4) $\times 10^{-7}$ M for cytochalasin B (Jung & Rampal, 1977) and (3–8) $\times 10^{-6}$ M for forskolin (Shanahan et al., 1987).

The fluorescence quenching induced by cytochalasin B and forskolin are qualitatively similar (Figure 4), although cytochalasin B gave a slightly greater maximal quenching (Table I). This apparent similarity disappears, however, when D-glucose is also present (Figures 1A and 5): Forskolin-induced fluorescence quenching is significantly reudced upon the addition of an excess of D-glucose (Figure 5), resulting in spectra similar to that seen with D-glucose alone (curve B of Figure 1). This finding was expected, as glucose competitively displaces forskolin binding (Shanahan et al., 1987) and forskolin gave much (2-fold) more quenching than D-glucose (Table I). Comparison of curve C with curve D in Figure 1A, however, shows that the fluorescence quenching induced by cytochalasin B is not reduced but increased at the shorter wavelengths by the addition of D-glucose. This is contrary to prediction from binding studies where glucose competes with cytochalasin B (Jung & Rampal, 1977; Baldwin & Henderson, 1989) and the fact that cytochalasin B quenches much (2.6-fold) more than D-glucose (Table I). For cytochalasin B-bound HEGT, excitation at 276 nm (Figure 2) gave much more quenching than excitation at 295 nm (Figure 1), indicating that tyrosine residues are strongly quenched by cytochalasin B. This may in part account for the fluorescence decrease at shorter wavelengths seen in Figure 1 in the presence of D-glucose plus cytochalasin B discussed above.

Internal Quenching of HEGT Fluorescence at Varying pH. Intrinsic tryptophan fluorescence in proteins is known to be sensitive to protonation or deprotonation of neighboring residues such as imidazolium of histidine (pK_a 5.6–7.0), the carboxyl groups of aspartic acid (pK_a 3.0–4.7) and glutamic acid (pK_a around 4.4), or the sulfhydryl of cysteine (pK_a 8.5–11) (Stryer, 1975; White et al., 1978). Figures 6 and 7 show the pH titration curves of the HEGT emission scans at 350 and 320 nm, respectively, with excitation at 295 nm, in the absence and presence of D-glucose, cytochalasin B, or forskolin. It is relevant to note that the cytochalasin B-binding activity of HEGT is not significantly affected by changes in pH between 3.5 and 9.0 (Jung et al., 1986).

The fluorescence of polar tryptophan(s) in unliganded HEGT was greatly affected by changes in pH between 4.5 and 6.5 with an apparant inflection point at around 5.5 (Figure 6). Approximately 25% of the fluorescence was quenched over

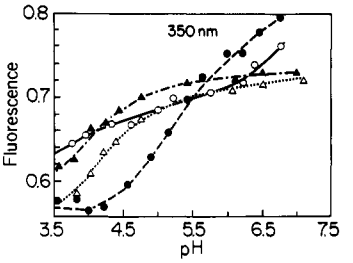

FIGURE 6: pH dependence of the intrinsic fluorescence of HEGT measured at 350-nm emission with 295-nm excitation. The pH titrations are in the absence (●) and in the presence of 400 mM D-glucose (○), 15 μM cytochalasin B (▲), or 15 μM forskolin (△).

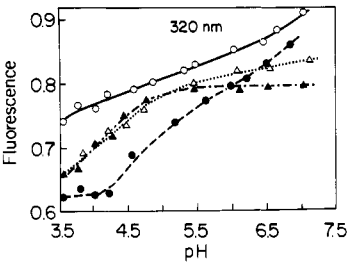

FIGURE 7: pH dependence of the intrinsic fluorescence of HEGT measured at 320-nm emission. Excitation was at 295 nm. The pH titrations are done in the absence (●) and in the presence of 400 mM D-glucose (○), 15 μM cytochalasin B (▲), and 15 μM forskolin (△).

this pH region (Figure 6). This suggests that at least one tryptophan is adjacent to a histidine residue and is quenched by its protonation. In contrast, in the presence of an excess of substrate or inhibitors, the fluorescence was little affected by changes over this pH region (Figure 6). This would suggest that the tryptophan has moved away from the histidine, or alternatively, that the tryptophan fluorescence is totally quenched by each of these ligands.

The 350-nm titration in Figure 7 also reveals steep changes in HEGT fluorescence over the pH range between 3.5 and 4.5, if cytochalasin B or forskolin is present, implying quenching by a carboxyl group. The fluorescence of either unliganded HEGT or D-glucose-bound HEGT was not affected, or was minimally affected, in this acidic pH region (Figure 6). These finding suggest that the inhibitors, but not the substrate, induce conformational changes where an exposed tryptophan becomes next to a carboxyl group.

The fluorescence titration at 320 nm (Figure 7) also shows similar pH quenching patterns as seen with the titration at 350 nm (Figure 6): Unliganded HEGT fluorescence was selectively quenched over the pH range of 4.5–6.5, while these of cytochalasin B- and forskolin-bound HEGT were affected significantly only over the pH range of 3.5–4.5. The titration of D-glucose-bound HEGT shows litle or no distinct quenching over the entire range of pH between 3.5 and 6.5, suggesting that the nonpolar tryptophan(s) is (are) not anywhere near the postulated carboxyl or histidine group. At pH 3.5–4.5, the fluorescence of glucose-bound HEGT is 15–20% higher compared with unliganded HEGT. This is consistent with our interpretation that D-glucose induces conformational changes which move a tryptophan to a nonpolar environment away from a polar region in HEGT (Figure 3).

The 350-nm titration from pH 7 to 9 (Figure 8) revealed quenching of a polar tryptophan in unliganded HEGT with a pK_a of approximately 8.4. This would suggest that one polar tryptophan is adjacent to a cysteine residue. The extent of this quenching is about 10–15% of the total fluorescence. The titration of cytochalasin B-bound HEGT shows a very similar quenching pattern as unbound HEGT, suggesting that the

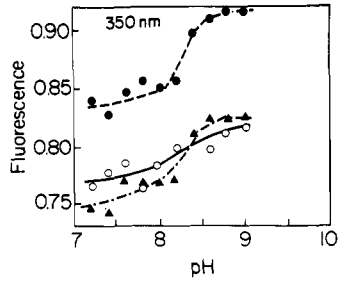

FIGURE 8: pH dependence of the intrinsic fluorescence of HEGT measured at 350-nm emission. Excitation was at 295 nm. The titrations are done in the absence (●) and in the presence of 400 mM D-glucose (○) and 15 μM cytochalasin B (▲).

inhibitor binding did not disrupt this tryptophan–cysteine interaction. In D-glucose bound HEGT, however, the quenching was considerably less, compared with unliganded or cytochalasin B-bound HEGT, indicating that the tryptophan residue is spending less or no time in the vicinity of this cysteine residue.

Discussion

Substrate-Induced Changes in HEGT Fluorescence. We show here for the first time that D-glucose induces a dose-dependent increase in nonpolar fluorescence in addition to the well-known reduction of polar fluorescence (Figures 1 and 3). This would indicate that D-glucose-induced conformational changes include the movement of a polar tryptophan to a nonpolar environment. The increase in nonpolar fluorescence is rather small at pH 7.4, most likely due to a low quantum yield of this nonpolar tryptophan at this pH. At a lower pH (Figures 1 and 7), the increase is as large as 20%. This increase is specific to D-glucose (Figures 1 and 7). The fact that the increase in nonpolar fluorescence and the quenching of polar fluorescence show two distinct dose dependencies (K_D) to glucose (Table I) simply indicates that the substrate-induced conformational changes essential to this protein function are more complex than a shift of a tryptophan residue from polar to nonpolar regions.

The D-glucose-induced conformational changes also include an exposure of new tyrosine residues that can be quenched by cytochalasin B (Figure 1) but not by forskolin (Figure 5). This effect on putative tyrosine is most likely due to quenching by free cytochalasin in solution although it could be due to bound cytochalasin B if the relaxation of glucose-induced conformation is slow (Frieden, 1978). This new finding may be useful to probe the segments involved in the conformational changes induced by D-glucose.

Effect of pH on HEGT Fluorescence. We demonstrate here that the intrinsic fluorescence of unliganded HEGT is affected in two discrete pH regions, pH 4.5–6.5 (Figure 7) and pH 7.0–9.0 (Figure 9). The changes are as large as 20% and 8% of the total intrinsic fluorescence, respectively (Figures 6 and 8). These suggest that at least two polar tryptophans are quenched, one most likely by a histidine imidazolium and the other by a cysteine sulfhydryl. We suggest that, in unliganded HEGT, one tryptophan is adjacent to a histidine, while the other is adjacent to a cysteine. When liganded by cytochalasin B or by forskolin, however, the pH sensitivity at the histidine region largely disappears, with the emergence of a new quenching between pH 3.5 and 4.5, while the quenching at the cysteine region remains largely intact (Figures 6, 7, 8). The new quenching at the acidic pH region suggests that one tryptophan is nearby a carboxyl group. When liganded with D-glucose, HEGT intrinsic fluorescence is much less sensitive to pH changes, and none of the putative histidine, cysteine, and carboxylic acid quenching is evident (Figures 6, 7, and 8).

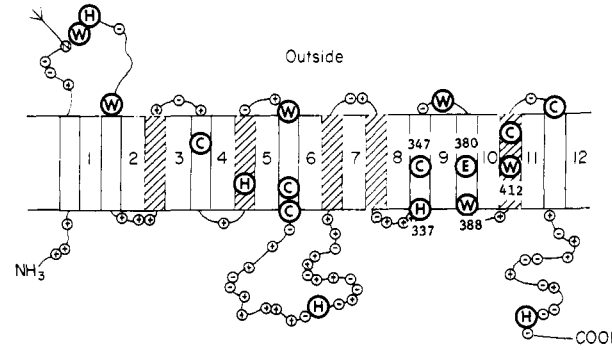

FIGURE 9: Relative positions of six tryptophan (W), six cysteine (C), and five histidine (H) residues of HEGT in its primary structure and transmembrane orientation deduced by hydropathy analysis according to Mueckler et al. (1985). Also shown is the relative position of Glu380 (E).

The Structure and Dynamics of HEGT: A Model. Definitive identification of the individual amino acids implicated in the pH quenching of HEGT described here is not possible at this time. Tentative identification of these residues, however, may be attempted on the basis of known structural information on this protein: There are only six tryptophan, six cysteine, and five histidine residues in this protein whose relative positions in the primary structure and in its transmembrane disposition (Mueckler et al., 1985) have been deduced (Figure 9). Furthermore, the substrate- and inhibitor-binding sites of HEGT are known to be located between TMH 7 and TMH 11, most likely somewhere in TMH 10 and TMH 11 (Holman & Rees, 1987), indicating the importance of these TMHs in the protein function. The TMHs adjacent in the primary structure are likely to be adjacent in the tertiary structure (Baldwin & Henderson, 1989), suggesting that TMHs 9, 10, and 11 are in juxtaposition in the tertiary structure of HEGT.

We propose as a working hypothesis that Trp388 of TMH 10 and Trp412 of TMH 11 are the two polar tryptophans responsible for the pH quenching discussed above. As indicated in Figures 9 and 10, His337, located just outside of TMH 9, can interact with Trp388, and Cys347 of TMH 9 also can be near Trp412, accounting for the quenching by histidine (Figure 6) and cysteine (Figure 8) protonation, respectively. Trp388 is located in TMH 10 close to its cytoplasmic end (Figures 9 and 10). Because of the proline-rich sequence that precedes it, Trp388 would stick out and thus make a contact with His337 in the cytosolic aqueous environment (Figure 10). It is also clear in Figures 9 and 10 that one can put Glu380 of TMH 10 close to Trp412 by a simple rotation of TMH 10. This would account for the proposed carboxyl quenching observed with cytochalasin B- or forskolin-liganded HEGT (Figures 6 and 7). Aspartic acid, the other carboxylic acid that may be responsible for the observed acidic quenching, is not found in the transmembrane segments.

The wheel plot of TMH 11 (not illustrated) shows that Trp412 is opposite the side containing the hydroxyl and amide residues lining the putative aqueous channel (Mueckler et al., 1985). This would allow Cys347 on TMH 9 contact Trp412 of TMH 11 for quenching to occur. Trp412, however, may be in a water pocket formed between TMHs 9, 10, and 11, which would provide a polar environment for this tryptophan.

Implicit in this model is that TMH 10 rotates upon substrate or inhibitor binding. The rotation induced by inhibitor binding would move Trp388 away from His337 and bring Glu380 of TMH 10 close to Trp412 of TMH 11, consistent with a

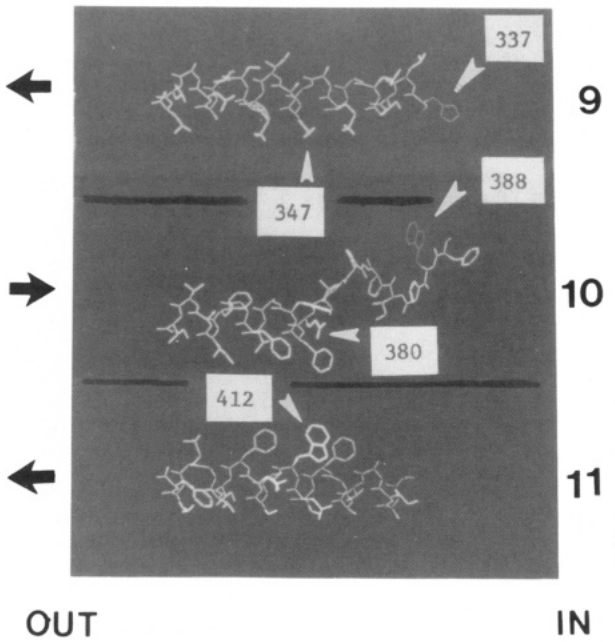

FIGURE 10: Molecular graphic representation of predicted relative positions of TMHs 9, 10, and 11 in HEGT. Individual TMHs 9, 10, and 11 are identified in right margin. The arrows in left margin indicate direction of amino acid sequences. Also shown at the bottom are extracellular (out) and intracytoplasmic (in) faces. Predicted secondary structures (determined as detailed under Materials and Methods) and transmembrane dispositions of TMHs are positioned to illustrate the juxtaposition of His337 (in TMH 9) and Trp388 (in TMH 10), and Cys347 (in TMH 9), Glu380 (in TMH 10), and Trp412 (in TMH 11).

dispparance of histidine quenching with a new carboxyl quenching (Figure 6). These findings suggest that cytochalasin B binding fixes the orientation of TMH 10 after the rotation. Furthermore, the cysteine quenching remains intact in the presence of cytochalasin B (Figure 8), indicating that Trp412 does not move with respect to Cys347 in TMH 9 upon cytochalasin binding. The substrate-induced TMH 10 rotation, on the other hand, is a dynamic oscillation and relaxes the overall interactions between TMHs 9, 10, and 11. The following facts support this conclusion: Glucose causes an increase in nonpolar tryptophan fluorescence with a reduction in polar fluorescence (Figure 3), abolishes the His337 protonation effect on Trp412 fluorescence, and fails to induce the Trp412 quenching by Glu380 (Figure 6).

All of the HEGT structural features predicted here are yet to be verified in future studies, including X-ray crystallography. Our model meanwhile will provide useful guidelines in designing biochemical and molecular biological experiments for the elucidation of the molecular mechanisms underlying this important protein function.

ACKNOWLEDGMENTS

We are grateful to Drs. M. Shibata and R. Rein of Roswell Park Research Institute for their help in computer graphic analysis. We are also grateful to Mrs. Carol Moronski for purification and reconstitution of HEGT.

Registry No. His, 71-00-1; Cys, 52-90-4; Trp, 73-22-3; glucose, 50-99-7; cytochalasin B, 14930-96-2; forskolin, 66575-29-9.

REFERENCES

Ahl, P. L., Stern, L. J., During, D., Mogi, T., Khorana, H. G., & Rothschild, K. J. (1988) *J. Biol. Chem. 263*, 13594–13601.

Applemann, J. R., & Lienhard, G. E. (1985) *J. Biol. Chem. 260*, 4575–4578.

Applemann, J. R., & Lienhard, G. E. (1989) *Biochemistry 28*, 8221–8227.

Baldwin, J. M., & Henderson, P. J. F. (1989) *Annu. Rev. Physiol. 51*, 459–471.

Baldwin, J. M., Gorga, J. C., & Lienhard, G. E. (1981) *J. Biol. Chem. 256*, 3685–3689.

Baldwin, S. A., Baldwin, J. M., & Lienhard, G. E. (1982) *Biochemistry 21*, 3836–3842.

Bartlett, G. R. (1959) *J. Biol. Chem. 234*, 469–471.

Bell, G. I., Kayano, T., Buse, J. B., Burant, C. F., Takeda, J., Lin, D., Fukumoto, H., & Seino, S. (1990) *Diabetes Care 13*, 198–208.

Birnbaum, M. J., Haspel, H. C., & Rosen, O. M. (1986) *Proc. Natl. Acad. Sci. U.S.A. 83*, 5784–5788.

Brandl, C. J., & Deber, C. M. (1986) *Proc. Natl. Acad. Sci. U.S.A. 83*, 917–921.

Brandl, C. J., Green, N. M., Korczak, B., & MacLennan, D. H. (1986) *Cell 44*, 597–607.

Cairns, M. T., Alvarez, J., Panico, M., Gibbs, A. F., Morris, H. R., Chapman, D., & Baldwin, S. A. (1987) *Biochim. Biophys. Acta 905*, 295–310.

Carruthers, A. (1986a) *J. Biol. Chem. 261*, 11028–11037.

Carruthers, A. (1986b) *Biochemistry 25*, 3592–3602.

Carruthers, A. (1990) *Physiol. Rev. 70*, 1133–1176.

Charron, M. J., Brosius, F. C., Alper, S. L., & Lodish, H. A. (1989) *Proc. Natl. Acad. Sci. U.S.A. 86*, 2535–2539.

Chen, R. F., & Edelhoch, H. (1975) *Biochemical Fluorescence*, Marcel Dekker, New York.

Chin, J. J., Jung, E. K. Y., & Jung, C. Y. (1986) *J. Biol. Chem. 261*, 9155–9160.

Chin, J. J., Jung, E. K. Y., Chen, V., & Jung, C. Y. (1987) *Proc. Natl. Acad. Sci. U.S.A. 84*, 4113–4116.

Chou, P. Y., & Fasman, G. D. (1978) *Adv. Enzymol. Relat. Areas Mol. Biol. 47*, 45–148.

Deziel, M. R., Jung, C. Y., & Rothstein, A. (1985) *Biochim. Biophys. Acta. 819*, 83–92.

Fischbarg, J., Liebovitch, L. S., & Koniarek, J. P. (1987) *Biochim. Biophys. Acta 898*, 266–274.

Frieden, C. (1978) *Annu. Rev. Biochem. 20*, 124–142.

Gibbs, A. F., Chapman, D., & Baldwin, S. A. (1988) *Biochem. J. 256*, 421–427.

Gibrat, J. F., Garnier, J., & Robson, B. (1987) *J. Mol. Biol. 198*, 425–443.

Gorga, F. R., & Lienhard, G. E. (1982) *Biochemistry 21*, 1905–1908.

Holman, G. D., & Rees, W. D. (1987) *Biochim. Biophys. Acta 897*, 395–405.

James, D. E., Strube, M., & Mueckler, (1989) *Nature 338*, 83–87.

Jung, C. Y., & Rampal, A. L. (1977) *J. Biol. Chem. 252*, 5456–5463.

Jung, E. K. Y., Chin, J. J., & Jung, C. Y. (1986) *J. Biol. Chem. 261*, 9155–9160.

Kasahara, M., & Hinkle, P. C. (1977) *J. Biol. Chem. 252*, 7384–7390.

Konev, S. V. (1967) in *Fluorescence and Phosphorescence of Proteins and Nucleic Acids* (Udenfriend, S., Ed.) pp 9–59, Plenum Press, New York.

Kyte, J., & Doolittle, R. F. (1982) *J. Mol. Biol. 157*, 105–132.

Lowry, O. H., Rosebrough, N. J., Farr, A. L., & Randall, R. J. (1951) *J. Biol. Chem. 193*, 265–275.

Maxfield, F. R., & Scheraga, H. A. (1976) *Biochemistry 15*, 5138–5153.

Mueckler, M., Caruso, C., Baldwin, S. A., Panico, M., Blench, I., Morris, H. R., Allard, W. J., Lienhard, G. E., & Lodish,

H. F. (1985) *Science 229*, 941–945.
Parker, C. A. (1968) *Photoluminescence of Solutions*, p 222, American Elsevier, Amsterdam.
Pawagi, A. B., & Deber, C. M. (1990) *Biochemistry 29*, 950–955.
Pinkofsky, H. B., Rampal, A. L., Cowden, M. A., & Jung, C. Y. (1978) *J. Biol. Chem. 253*, 4930–4937.
Rampal, A. L., & Jung, C. Y. (1987) *Biochim. Biophys. Acta 896*, 287–294.
Rampal, A. L., Jung, E. K. Y., Chin, J. J., Deziel, M. R., Pinkofsky, H. B., & Jung, C. Y. (1986) *Biochim. Biophys. Acta 859*, 135–142.
Shanahan, M. F., Morris, D. P., & Edwards, B. M. (1987) *J. Biol. Chem. 262*, 5978–5984.
Sogin, D. C., & Hinkle, P. C. (1978) *J. Supramol. Struct. 8*, 447–453.
Stein, W. D. (1986) in *Transport and Diffusion Across Cell Membranes*, p 355, Academic Press, Inc., Orlando, FL.
Stryer, L. (1975) in *Biochemistry*, p 86, W. H. Freeman, San Francisco.
Tanford, C. (1982) *Proc. Natl. Acad. Sci. U.S.A. 79*, 2882–2884.
Weber, G., & Teal, F. W. J. (1965) *Proteins (2nd Ed.) 3*, 445.
Wheeler, T. J., & Hinkle, P. C. (1981) *J. Biol. Chem. 256*, 8907–8914.
White, A., Handler, P., Smith, E. L., Hill, R. L., & Lehman, I. R. (1978) in *Principles of Biochemistry*, 6th ed., p 107, McGraw-Hill, New York.

Structural Analysis of the Operator Binding Domain of Tn10-Encoded Tet Repressor: A Time-Resolved Fluorescence and Anisotropy Study

Marie Chabbert,[‡] Wolfgang Hillen,[§] Dieter Hansen,[§,∥] Masayuki Takahashi,[⊥] and Jean-Alain Bousquet*[,‡]

CNRS UA 491, Laboratoire de Physique, Faculté de Pharmacie de Strasbourg, BP 24, F-67401 Illkirch, France, Groupe de Cancérogénèse et de Mutagénèse Moléculaire et Structurale, IBMC du CNRS et Université Louis Pasteur, 15 rue René Descartes, F-67084 Strasbourg, France, and Lehrstuhl für Mikrobiologie, Institut für Mikrobiologie und Biochemie der Friedrich-Alexander Universität, Erlangen-Nürnberg, Staudtstrasse 5, G-8520 Erlangen, Federal Republic of Germany

Received May 31, 1991; Revised Manuscript Received November 22, 1991

ABSTRACT: An engineered Tn10-encoded Tet repressor, bearing a single Trp residue at position 43, in the putative α-helix–turn–α-helix motif of the operator binding domain, was studied by time-resolved fluorescence and anisotropy. Fluorescence intensity decay data suggested the existence of two classes of Trp-43, defined by different lifetimes. Analysis of anisotropy data were consistent with a model in which each class was defined by a different lifetime, rotational correlation time, and fluorescence emission maximum. The long-lifetime class had a red-shifted spectrum, similar to that of tryptophan zwitterion in water, and a short rotational correlation time. In contrast, the spectrum of the short-lifetime class was blue-shifted 10 nm compared to that of the long-lifetime class. Its correlation time was similar to that of the protein, which showed that Trp in this class was entirely constrained. Trp in this latter class could not be quenched by iodide, whereas most of the long-lifetime class was easily accessible. Presence of disruptive agents, such as 1 M GuCl or 3 M KCl, did not alter markedly the lifetimes but increased the weight of the short-lifetime component. In the same time, the rotational correlation time of this component was dramatically reduced. Taken together, our data suggest that the long-lifetime class could correspond to the tryptophan residues exposed to solvent whereas the short-lifetime class would correspond to the tryptophan residues embedded inside the hydrophobic core holding the helix–turn–helix motif. Destabilization of hydrophobic interactions would lead to an increase in the weight of the latter class for entropic reasons. Analysis of the fluorescence parameters of Trp-43 could provide structural information on the operator binding domain of Tet repressor.

Regulation of gene expression in procaryotes is often mediated by proteins which recognize DNA sequence specifically (Pabo & Sauer, 1984). The ability of many regulatory proteins to recognize the respective target DNA depends on the presence, e.g., Trp repressor (Gunsalus & Yanofsky, 1980), or the absence of effector molecules, e.g., Lac repressor (Miller & Reznikoff, 1980). X-ray analyses of the crystal structure of several repressors provide keys to the molecular basis of sequence specificity in DNA binding proteins. These data reveal that an α-helix–turn–α-helix structural motif is a common feature for sequence-specific DNA recognition among procaryotic DNA binding proteins (Pabo & Sauer, 1984). This α-helix–turn–α-helix motif makes sequence-specific contacts in the major groove of B-DNA. In this model, sequence specificity is achieved by interactions of amino acid side chains with solvent-exposed functions of the base pairs (Pabo & Sauer, 1984; Harrison & Aggarval, 1990).

Tet repressor controls transcription of the Tn10-encoded *tet* genes conferring resistance to tetracycline in Gram-negative bacteria (Beck et al., 1982; Bertrand et al., 1983; Hillen et al., 1984). This control is negatively regulated by the antibiotic tetracycline (Yang et al., 1976), which functions as an inducer (Hillen et al., 1983, 1984). Tet repressor has been purified and characterized (Hillen et al., 1982; Oehmichen et al., 1984) and its sequence has been determined (Postle et al., 1984). The comparison of Tet repressor with other repressor sequences (Pabo & Sauer, 1984) and the positions of trans-dominant mutations with reduced operator binding affinity (Isackson

[‡] Faculté de Pharmacie de Strasbourg.
[§] Institut für Mikrobiologie und Biochemie der Friedrich-Alexander Universität.
[∥] Present address: Henkel KGaA, TFB Biotechnologie, Henkelst. 67, G-4000 Düsseldorf, FRG.
[⊥] IMBC du CNRS et Université Louis Pasteur.

0006-2960/92/0431-1951$03.00/0